

# Localization transition in the Mermin model

Gregory Levine

*Department of Physics, Hofstra University, Hempstead, NY 11550*

*and*

*Department of Physics, Brookhaven National Laboratory, Upton, NY 11973-5000*

V. N. Muthukumar

*Joseph Henry Laboratories of Physics, Princeton University, Princeton, NJ 08544*

(March 22, 2022)

We study the dynamical properties of the Mermin model, a simple quantum dissipative model with a monochromatic environment, using analytical and numerical methods. Our numerical results show that the model exhibits a second order phase transition to a localized state before which the system is effectively decoupled from the environment. In contrast to the spin-boson model, the Mermin model exhibits an “orthogonality catastrophe,” defining the critical point, before dissipation has destroyed all coherent behavior. An analytic approach based on the Liouvillian technique, though successful in describing the phase diagram of spin-boson and related models, fails to capture this essential feature of the Mermin model.

PACS numbers: 03.65.Bz, 42.50.Lc

## I. INTRODUCTION

The formal analogies between phase transitions in one-dimensional systems, decoherence in the spin-boson Hamiltonian (SBH), and screening in Kondo systems have been important in sorting out the subtle behavior of dissipative quantum systems. In this paper we undertake an analytic and numerical study of the Mermin model, a model closely related to the spin-boson model, but possessing a monochromatic environmental spin bath.

The spin-boson model is a universal model for a two level system interacting weakly with an environmental bath, which has a continuous spectrum [1]. Although both monochromatic and polychromatic baths bring about a localization transition in the two level system, we point out, in this paper, an important difference between the dynamics of the two level system interacting weakly with these two kinds of baths. If the dynamics of the two level system is characterized by a (pseudo) spin susceptibility, increasing the coupling to the environment broadens the resonance and shifts the resonant frequency somewhat. When the environment has a continuous and ohmic spectrum (the SBH), the system spin first loses all coherent behavior at some intermediate coupling strength. The dynamics of the two level system becomes overdamped at this point, but the localization transition does *not* occur until a stronger coupling is reached. The

critical coupling at which the two level system is ultimately localized may be identified with an “orthogonality catastrophe.” Thus, before the environmental overlap effects become catastrophic, they are *finite* and lead to a continuous softening of the system energy scale, as well as a complete inelastic broadening to an incoherent state (the so called “Toulouse point”).

On the other hand, when the spectrum of the environment is monochromatic (the Mermin model), the resulting dynamics are different. As the coupling to the environment increases, the only effect is to broaden the coherent resonance. At a critical coupling, a redistribution of spectral weight is initiated and spectral weight flows from the coherent resonance to a localized feature at zero frequency. For coupling strengths beyond this value, spectral weight is increasingly transferred from the resonant peak to the localized feature. Thus, unlike the SBH, the Mermin model does not show any overdamped feature before the localization transition sets in. When localization does set in (at the critical point), *the coherent peak continues to exist, albeit with reduced spectral weight.* This is our main result.

The paper is organized as follows. In section II, we introduce the Mermin model and study the dynamics of the model using an analytical technique. This technique (based on Liouvillian operator methods) has been applied successfully in the past, to a variety of dissipative models, including the SBH. In section III, we study the model numerically, and show that the model exhibits a localization transition at a critical value of the coupling strength. The final section contains some concluding remarks, summarizing our results and suggesting future directions of study.

## II. LIOUVILLIAN DYNAMICS OF THE MERMIN MODEL

In this section, we introduce the Mermin model and study the dynamics of the model analytically. The model introduced by Mermin is obtained from the well known spin-boson Hamiltonian, by retaining only the lowest two levels of each harmonic oscillator comprising the environmental bath [2]. The Hamiltonian therefore describes a

“system” spin-1/2, represented by the Pauli matrices  $\sigma$ , coupled to a set of  $N$  “environment” spin-1/2 degrees of freedom,  $\{s_j\}$ . The resulting Hamiltonian, called the Mermin model is given by

$$H = -\frac{\Delta}{2}\sigma_x + \frac{\lambda}{4N}\sigma_z \sum_{j=1}^N (s_j^+ + s_j^-) + \frac{\omega}{2N} \sum_{j=1}^N s_j^z . \quad (1)$$

In this paper, we investigate a large  $N$  variant of the model (1). As first noted by Mermin, the model can be solved approximately in the  $N \rightarrow \infty$  limit, to demonstrate the correspondence between the onset of localization of the system spin and a second order phase transition [2]. In this large  $N$  model, the environment spins are summed to one big  $O(N)$  spin,  $\mathbf{S}$ , and contributions from the sectors of Hilbert space with total spin  $S < N/2$  are ignored. The Hamiltonian then becomes

$$H = -\frac{\Delta}{2}\sigma_x + \frac{\lambda}{2N}\sigma_z S_x + \frac{\omega}{2N}S_z . \quad (2)$$

As Mermin points out, the advantage of the Hamiltonian (2) is that in the limit  $N \rightarrow \infty$ , the environment spins may be replaced in the Hamiltonian by the  $x$  and  $z$  components of a classical spin angular momentum:  $\frac{\lambda}{N}\sigma_z S_x \rightarrow \frac{1}{2}\lambda\sigma_z \sin\theta$  and  $\frac{\omega}{N}S_z \rightarrow -\frac{1}{2}\omega \cos\theta$ . The resulting Hamiltonian may be diagonalized and its ground state eigenvalue,  $E_0(\theta)$ , given by

$$E_0(\theta) = -\frac{1}{2}\sqrt{\Delta^2 + \frac{\lambda^2}{4}\sin^2\theta} - \frac{\omega}{4}\cos\theta , \quad (3)$$

minimized with respect to  $\theta$ .

The critical behavior of the model may now be seen by examining the ground state energy  $E_0$ , as a function of  $\Delta$ . The ground state energy,  $E_0$ , bifurcates at a finite value of  $\Delta$  going from a singlet, non-degenerate root for  $\Delta > \lambda^2/2\omega$  to a doubly degenerate set for  $\Delta < \lambda^2/2\omega$ :

$$\begin{aligned} \theta_0 &= 0 & \Delta > \lambda^2/2\omega \\ \sin\theta_0 &= \pm\sqrt{\frac{1 - 4\Delta^2\omega^2/\lambda^4}{1 + \omega^2/\lambda^2}} & \Delta < \lambda^2/2\omega \end{aligned}$$

In the former case, the environment is decoupled from the system and always points along the  $z$ -axis to minimize its “Zeeman” energy corresponding to the last term of (2). In the latter case, the environment and the system spins are frozen in two distinct orientations with degenerate energies. The ground state wave function is still in a superposition  $\alpha|+\rangle + \beta|-\rangle$ , but is no longer an evenly weighted one ( $\alpha = \beta$ ); rather, the two roots correspond to the system predominantly in  $|+\rangle$  or  $|-\rangle$ .

Despite producing a localization transition, this mean field solution is necessarily incomplete, for, it ignores quantum fluctuations of the bath; *i.e.*, it provides no mechanism for dissipation. As a first step in this direction, we study the dynamics of the bath using the Liouillian operator method. This method has been applied

successfully to study a wide variety of dissipative systems. Using the Liouillian approach, Shao and Hänggi [3] studied a spin-spin bath system similar to the Hamiltonian (1) above, but with an ohmic spectrum and found a phase diagram virtually identical to that of the SBH. Dattagupta et al [4], studying the SBH, also employed a Liouillian approach and found close agreement with other analytic approaches to the SBH [1,5].

To try to gain some insight into the Mermin model beyond the mean field level, we have adapted the resolvent operator calculation of Shao and Hänggi [3] on the spin-spin bath model. In what follows, we just outline the basic steps in the calculation and describe our results. A detailed review of the resolvent operator formalism can be found elsewhere [6].

The Hamiltonian (2) is rotated by  $R \equiv \exp -i\sigma_z\theta_0 S_y$  to diagonalize the environment spin for the two orientations of the system spin. We then get

$$H' = -\frac{\Delta}{2}(s^+ e^{-2i\theta_0 S_y} + s^- e^{+2i\theta_0 S_y}) - \frac{(\omega^2 + \lambda^2)^{1/2}}{2N} S_z . \quad (4)$$

To study the dynamics of the system spin, a suitable quantity to calculate is  $\langle\sigma_z(t)\rangle$  where  $\langle\dots\rangle$  denotes quantum average at zero temperature. For a state prepared initially at  $t = 0$ , with the system and environment spin fully polarized, the time dependent average of the system spin is given by

$$p(t) = \langle S \uparrow | R^\dagger \sigma_z(t) R | \uparrow S \rangle ,$$

where the first index of the ket is the system state and the second is the environment. The spin operator  $\sigma_z(t)$  is in the Heisenberg representation, and its time evolution is governed by the transformed Hamiltonian,  $H'$ . We now introduce the Liouillian time evolution operator  $L$ , which is defined generically for a Hamiltonian  $H$ , Hilbert space  $\{|j\rangle\}$  and operator  $O$  as follows:

$$\langle i | O(t) | j \rangle = \sum_{i', j'} \langle i j | e^{iLt} | i' j' \rangle \langle i' | O(0) | j' \rangle .$$

The time evolution operator  $Q(t) \equiv \exp(iLt)$  is a fourth rank operator whose state space vectors are denoted by a ket-parenthesis,  $|ij\rangle$ . All dynamical information is contained in  $Q$  and the Laplace transform of  $Q$

$$(j\mu k\nu | Q(z) | l\mu' m\nu') \equiv (j\mu k\nu | \frac{1}{z - iL} | l\mu' m\nu') ,$$

is the most convenient form to calculate. For the initial conditions specified above, it follows that the Laplace transform of  $p(t)$  is given by:

$$p(z) = \sum_{m\mu jk} \alpha_j \alpha_k^* (k \uparrow j \uparrow | Q(z) | m\mu m\mu) \mu \quad (5)$$

where the  $\alpha$ 's are the rotation group matrix elements,

$$\alpha_j \equiv \langle j \uparrow | R | \uparrow S \rangle$$

Following Dattagupta *et al.* [4], we concentrate on the “environment-averaged” time evolution operator defined by performing the environment sums in (5)

$$(\mu\nu | \langle Q(z) \rangle | \mu' \nu') \equiv \sum_{kjm} \alpha_j \alpha_k^* (k\mu j \nu | Q(z) | m \mu' m \nu')$$

The Liouvillian is now split into perturbation ( $L_i$ ) and environment ( $L_e$ ) parts, corresponding to the two terms in equation (4). Then the environment averaged time development operator may be computed perturbatively as

$$(\mu\nu | \langle Q(z) \rangle | \mu' \nu') = (\mu\nu | \frac{1}{z - \langle M \rangle_c} | \mu' \nu') , \quad (6)$$

where

$$\begin{aligned} (\mu\nu | \langle M \rangle_c | \mu' \nu') &= z(\mu\nu | \langle iL_i G \rangle | \mu' \nu') \\ &\quad - z(\mu\nu | \langle L_i G L_i G \rangle | \mu' \nu') \\ &\quad + z(\mu\nu | \langle L_i G \rangle^2 | \mu' \nu') + \dots , \end{aligned} \quad (7)$$

and  $G$  is the Liouvillian propagator for the environment degrees of freedom,  $G^{-1} = z - iL_e$ .

We can now calculate the above terms. The results through second order in  $\Delta$  for the three self-energies in the order appearing in equation (7) (notated  $M_1$ ,  $M_{21}$ ,  $M_{22}$ ) are given below:

$$M_1 = i\Delta \langle S | R^2 | S \rangle (\delta \otimes \sigma^x - \sigma^x \otimes \delta) \quad (8)$$

$$\begin{aligned} M_{21} &= -\frac{1}{2} B(z) \delta \otimes (\delta + \sigma^z) - \frac{1}{2} B^*(z) (\delta + \sigma^z) \otimes \delta \\ &\quad - \frac{1}{2} C(z) \delta \otimes (\delta - \sigma^z) - \frac{1}{2} C^*(z) (\delta - \sigma^z) \otimes \delta \\ &\quad + \frac{1}{2} (B(z) + B^*(z)) S^- \otimes S^- \\ &\quad + \frac{1}{2} (C(z) + C^*(z)) S^+ \otimes S^+ \end{aligned} \quad (9)$$

$$M_{22} = \frac{1}{2} \frac{\Delta^2}{z} |\langle S | R^2 | S \rangle|^2 (\delta \otimes \delta - \sigma^x \otimes \sigma^x) \quad (10)$$

The outer product notation  $\alpha \otimes \beta$  corresponds to  $\alpha_{\mu\mu'} \beta_{\nu\nu'}$ . The  $z$  dependences of  $M_{21}$  are given by

$$\begin{aligned} B(z) &= \frac{\Delta^2}{4} \sum_{kn} \frac{1}{z - i\epsilon_{kn}} \langle n | R^3 | S \rangle \langle S | R^\dagger | k \rangle \langle k | R^{\dagger 2} | n \rangle \\ C(z) &= \frac{\Delta^2}{4} \sum_{kn} \frac{1}{z - i\epsilon_{kn}} \langle n | R^\dagger | S \rangle \langle S | R^\dagger | k \rangle \langle k | R^2 | n \rangle \end{aligned}$$

where  $\epsilon_{kn} \equiv \epsilon_k - \epsilon_n$  is the bare energy difference. The fluctuation matrix elements are depicted graphically in

Fig. (1). Since  $\epsilon_k - \epsilon_n$  depends only upon  $k - n$ ,  $n \equiv k + r$ , may be written in terms of a relative index  $r$  and the  $k$  sum performed. For large  $S$ , the matrix elements, as functions of  $r$ , are peaked at the most probable values of  $r$ . Now, the two self energies may be written in the large  $S$ , continuum limit as follows:

$$\begin{aligned} \text{Re}C(z) &= \frac{\Delta^2}{2\lambda\sqrt{\pi}} \int_{-\infty}^{\infty} d\epsilon \frac{z}{z^2 + \epsilon^2} e^{-\left(\frac{\epsilon}{\lambda}\right)^2} \\ \text{Re}B(z) &= \frac{\Delta^2}{2\lambda\sqrt{\pi}} \int_{-\infty}^{\infty} d\epsilon \frac{z}{z^2 + \epsilon^2} e^{-\left(\frac{\epsilon - \bar{\epsilon}}{\lambda}\right)^2} \end{aligned}$$

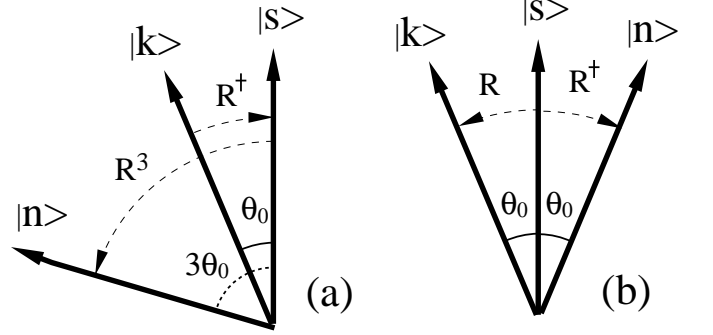


FIG. 1. Fluctuation matrix elements depicted for processes contributing to  $B(z)$  and  $C(z)$ .

These self energies cannot be calculated in closed form; however, they can be evaluated in several limits that are physically significant. For  $C(z)$  we find,

$$\begin{aligned} \text{Re}C(z) &\sim \frac{\Delta^2}{\lambda} \quad z \ll \lambda \\ \text{Re}C(z) &\sim \frac{\Delta^2}{z} \quad z \gg \lambda \text{ or } \lambda \ll \omega \end{aligned}$$

and for  $B(z)$ ,

$$\begin{aligned} \text{Re}B(z) &\sim \frac{\Delta^2}{\lambda} e^{\bar{\epsilon}^2/\lambda^2} \quad z \ll \lambda \\ \text{Re}B(z) &\sim \Delta^2 \frac{z}{z^2 + \bar{\epsilon}^2} \quad \lambda \ll \omega \\ \text{Re}B(z) &\sim \frac{\Delta^2}{z} \quad z \gg \lambda \end{aligned}$$

where  $\bar{\epsilon} = \omega(\cos \theta_0 - \cos 3\theta_0)$ .

To compute the Laplace transform of  $p(t)$  the self energies (8), (9), and (10) must be inserted in eqn. (6) and the fourth rank operator inverted. The general form is complicated, but for small  $z$ , the analytic structure reduces to

$$p(z) = \frac{\text{Re}C(z) + z}{z(z + \text{Re}C(z) + \text{Re}B(z))} .$$

In the limit of large environmental coupling, the real pole dominates and the behavior for  $p(t)$  is exponential decay; at zero temperature, the system prepared in one state will leak into the other state. Thus, we get,

$$p(t) = e^{-t\Delta^2/\lambda} \quad \lambda \gg \Delta \quad (11)$$

For small environmental coupling, the pole in  $p(z)$  is imaginary and  $p(t)$  oscillates, given by

$$p(t) = \cos \Delta t \quad \lambda \ll \Delta \quad (12)$$

The results Eq. (11) and (12) summarize the two extremal behaviors of  $p(t)$ , but give no information about the critical point between.

### III. NUMERICAL RESULTS FOR THE MERMIN MODEL

There are two main differences between the predictions of the Liouvillian perturbative scheme and the exact numerical behavior. First, the Liouvillian formalism does not capture the phase transition observed in finite size scaling of the numerical results (as well as in the mean field solution) described below. This result is interesting, given that the Liouvillian formalism does describe the phase transition at  $\alpha = 1$  of the spin-boson [4] and spin-spin bath [3] models. Consequently, one would expect it to work for the simpler monochromatic spectrum of the Mermin model. Secondly, the Liouvillian formalism predicts exponential decay in  $p(t) \sim e^{-t\Delta^2/\lambda}$  for large environmental coupling  $\lambda$ . The corresponding spectral function is Lorentzian centered at  $\nu = 0$ , similar to that of the spin-boson model at the Toulouse point  $\alpha = 1/2$ . However, in our numerical results we will show that the spectral function has only a finite energy ( $\sim O(\Delta)$ ) feature and an exponentially small frequency ( $\sim O(\Delta e^{-N/2})$ ) delta function feature (for environmental coupling larger than the critical value.)

Let us now summarize briefly, our numerical findings. The transition to decoherence is induced by strong coupling to environmental degrees of freedom (large  $\lambda$ ), or, equivalently, a small system energy scale (small  $\Delta$ ). Below a critical coupling,  $\lambda_c$ , all spectral weight of the dynamical susceptibility

$$\chi''(\nu) \equiv \text{Im} \frac{i}{4} \int_{-\infty}^{\infty} dt \langle 0 | [\sigma(t), \sigma(0)] | 0 \rangle \theta(t) e^{i\nu t} \quad (13)$$

resides in the principal resonance of the two level system at an energy  $\Delta$ . When the coupling is larger than  $\lambda_c$ , a new exponentially small energy scale  $O(\Delta e^{-N/2})$  emerges, associated with a broken symmetry,  $\langle \sigma \rangle \neq 0$ , in the thermodynamic limit  $N \rightarrow \infty$ . This feature corresponds to tunneling modified by a Franck-Condon

type overlap factor. As the coupling is increased, spectral weight is shifted continuously to the “near-zero” frequency channel. The weight of the delta-function,  $\delta(0^+)$ , is simply the order parameter,  $|\langle 0 | \sigma | 0 \rangle|^2$  (or, more exactly,  $|\langle 1 | \sigma | 0 \rangle|^2$ , for large but finite  $N$ ). However, the dynamical susceptibility obeys a sum rule, implying that an incompletely formed broken symmetry state leaves some spectral weight at the position of the principal resonance, set by  $\Delta$ .

To calculate the dynamical susceptibility we consider the response of the system (2) to an external field  $h(t) = h \cos \nu t$ :

$$H_{\text{ext}} = -h \frac{\sigma_z}{2} \cos \nu t \quad (14)$$

The Hamiltonian (2) was diagonalized and the complete order parameter matrix,  $\sigma_{ij} \equiv \langle i | \sigma | j \rangle$ , was computed. It is natural to work with the dimensionless coupling constant,  $\kappa \equiv 2\omega\Delta/\lambda^2$ ; The critical coupling implied in the  $N \rightarrow \infty$  calculation is then  $\kappa = \kappa_c = 1$ .

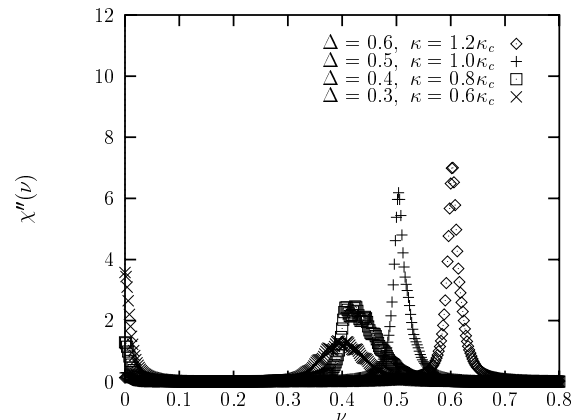


FIG. 2. Evolution of spectral weight in the Mermin Model.  $\chi''(\nu)$  is shown for four values of  $\kappa$  decreasing below the critical value,  $\kappa_c$ . Despite the change in the position of the principal resonance (due to changing  $\Delta$ ), spectral weight emerges at  $\nu \sim 0$  abruptly at  $\kappa_c$  and the two features remain distinct.

Fig. (2) shows the behavior of  $\chi''(\nu)$  as the system energy scale  $\Delta$  is reduced, corresponding to a range  $\kappa = 0.6\kappa_c - 1.2\kappa_c$ . These computations were performed for  $N = 80$ . Computations on larger spin environments (up to  $N = 300$ ) suggest that there is little change beyond  $N = 80$ . An artificial broadening ( $\delta = 0.01$ ) was added to make the features more visible. As seen in this sequence,  $\kappa = \kappa_c$  is marked by the appearance of the Franck-Condon resonance at an exponentially small energy scale ( $\nu_{10} \sim 10^{-3}$ ). The spectral weight remaining at  $O(t)$  when  $\kappa > \kappa_c$  clearly exhibits inelastic broadening, although the resonance essentially disappears before becoming critically damped.

The counterpart, at finite  $N$ , to  $\langle \sigma \rangle \neq 0$  at infinite  $N$  is the spectral weight at the Franck-Condon resonance,  $\sigma_{10} \neq 0$ . Fig. 3 demonstrates that  $\sigma_{10}$  behaves as expected in a second order phase transition; the slope at  $\kappa = \kappa_c^+$  grows with increasing  $N$ . The matrix,  $\sigma_{ij}$ , and consequently,  $\chi''(\nu)$ , obey a sum rule:

$$\sum_i |\sigma_{ij}|^2 = 1 \quad (15)$$

An incompletely developed broken symmetry ( $|\sigma_{10}|^2 < 1$ ) means that spectral weight remains at the principal resonance at  $O(\Delta)$ .

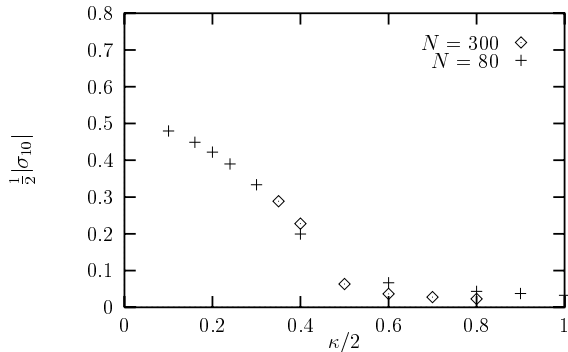


FIG. 3. The order parameter,  $\sigma_{10}$ , is plotted as a function of  $\kappa$  and exhibits second order phase transition behavior.  $\kappa$  was varied by changing  $\Delta$ . Comparison of  $N = 80$  and  $N = 300$  data show the slope steepening at the critical point. When  $\kappa > \kappa_c$ , there is no weight in the Franck-Condon resonance other than that attributed to the rounding of the phase transition at finite  $N$ .

The quantum fluctuations missed by the mean field analysis but captured in the numerics may be qualitatively divided into two types: overlap effects and inelastic effects. In the former type, the system in the  $|+\rangle$  state leaves an “imprint” upon the environment which, being nearly orthogonal to the imprint left by system state  $|-\rangle$ , reduces the tunneling amplitude by an exponentially small factor. The new tunnel splitting is thus reduced by a Franck-Condon type overlap factor:

$$\Delta^* = \Delta \langle \theta_0 | R_y(2\theta_0) | \theta_0 \rangle = \Delta \cos^N \theta_0 = \Delta \frac{1}{(1 + \lambda^2/\omega^2)^{N/2}} \quad (16)$$

where  $R_y(2\theta_0)$  is the rotation operator. The resonance then shifts from  $O(\Delta)$  to a smaller energy scale  $O(\Delta e^{-N/2})$ . In the inelastic type fluctuation, the system forces the environment to make transitions to an excited state dissipating an amount energy  $\lambda^2/\omega$  per period. The resonance is then broadened by  $O(\lambda^2/\omega)$  but remains nominally at  $O(\Delta)$ .

These results show that the spin dynamics of the Mermin model is significantly different from that of the SBH with an ohmic bath. The former, as our results show, only exhibits overlap effects at the critical coupling, but not before. In the SBH, the coupling to the environment produces *finite* overlap effects for all couplings  $0 < \alpha < 1/2$ , and a Franck-Condon type reduction in energy scale, given by:

$$\Delta_{\text{eff}} = \Delta \left( \frac{\Delta}{\omega_c} \right)^{\frac{\alpha}{1-\alpha}}. \quad (17)$$

At the same time, inelastic effects decohere the resonance leading to the Toulouse limit (at  $\alpha = 1/2$ ), prior to localization (which occurs at  $\alpha = 1$ ), and corresponding to a complete inelastic broadening of the resonance. [7–9]. In the Mermin model, the quantum resonance of the system spin, although damped, remains intact through the localization transition.

#### IV. CONCLUSION

In this paper we have compared the dynamical behavior of a quantum dissipative system possessing a monochromatic spectrum (the Mermin model) with that of the spin-boson model which possesses a continuous bath spectrum. We find an important difference between the dynamical behavior of the two models, with the Mermin model reaching a localized state, as environmental coupling is increased, without the primary resonance becoming overdamped. When the critical coupling is reached, spectral weight is transferred across a gap of  $O(\Delta)$  to a zero frequency delta function, indicating the presence of a localized state. In effect, the Mermin model exhibits no *finite* environmental overlap effects until an infinite one—the orthogonality catastrophe—localizes the system. In contrast, the primary resonant feature in spin-boson model must soften to zero frequency and become completely overdamped (the Toulouse point  $\alpha = 1/2$ ) before a localized spectral feature appears at  $\alpha = 1$ . Furthermore, the Liouvillian technique, which has been successful in capturing the localization phase transition in the SBH and related models fails for the Mermin model.

The Mermin model is a prototype system for a weakly coupled  $O(1/N)$  monochromatic spin bath, and judging from the results of Hanggi, a weakly coupled monochromatic *oscillator* bath is likely to exhibit the same behavior. In contrast, the spin-boson model employs a featureless, power-law spectrum of environmental oscillators and exhibits universal behavior that depends only upon the exponent of the spectrum. This behavior, in the ohmic case, includes a localization transition, but one with a qualitatively different character than that of the Mermin model. It is natural, then, to ask under what conditions does a quantum environment become sufficiently

“featureless” to fit into the universal framework of the spin-boson model?

### ACKNOWLEDGMENTS

G.L. gratefully acknowledges the support of the Cottrell Foundation through Research Corporation Grant number CC3834. Work performed at BNL supported by the U.S. DOE under contract no. DE-AC02 98CH10886. V.N.M. is supported by NSF Grant DMR-9104873.

---

- [1] See A. J. Leggett, S. Chakravarty, A. T. Dorsey, Matthew P. A. Fisher, Anupam Garg, and W. Zwerger, *Rev. Mod. Phys.* **59**, 1 (1987) and references therein.
- [2] N. D. Mermin, *Physica A* **177**, 561 (1991). See also G. Levine, *Phys. Rev.* **B61**, 4636 (2000).
- [3] J. Shao and P. Hänggi, *Phys. Rev. Lett.* **81**, 5710 (1998).
- [4] S. Dattagupta, H. Grabert, and R. Jung, *J. Phys.: Condens. Matter* **1**, 1405 (1989).
- [5] U. Weiss *Quantum Dissipative Systems*, (World Scientific 1999), page 338.
- [6] S. Dattagupta *Relaxation Phenomenon in Condensed Matter Physics* (Academic Press 1987).
- [7] J. T. Stockburger and C. H. Mak, *Phys. Rev. Lett.* **80**, 2657 (1998).
- [8] F. Lesage, H. Saleur and S. Skorik, *Phys. Rev. Lett.* **76**, 3388 (1996).
- [9] T. A. Costi and C. Kieffer, *Phys. Rev. Lett.* **76**, 1683 (1996).